Gallo, Pasquale; Hagiwara, Yohei; Shimada, Takahiro; Kitamura, Takayuki

Strain energy density approach for brittle fracture from nano to macroscale and breakdown of continuum theory

Published in:
Theoretical and Applied Fracture Mechanics

DOI:
10.1016/j.tafmec.2019.102300

Published: 04/07/2019

Document Version
Early version, also known as pre-print

Strain energy density approach for brittle fracture from nano to macroscale and breakdown of continuum theory

Pasquale Gallo[a,b *], Yohei Hagiwara[a], Takahiro Shimada [a], Takayuki Kitamura[a]

[a] Kyoto University, Department of Mechanical Engineering and Science, Kyoto-daigaku-Katsura, Nishikyo-Ku, Kyoto 615-8540, Japan
[b] Aalto University, School of Engineering, Department of Applied Mechanics, P.O. Box 14300, FIN-00076 Aalto, 02150 Finland

*Corresponding author: pasquale.gallo@aalto.fi

Abstract

In contrast to the great success at the macroscale, fracture mechanics theory fails to describe the fracture at a critical size of several nanometers due to the emerging effect of atomic discreteness with decreasing material size. Here, we propose a novel formulation for brittle fracture, from macro- to even atomic scales, based on extended strain energy density, and give an insight into the breakdown of continuum theory. Numerical experiments based on molecular statistics (MS) simulations are conducted on single-edge cracked samples made of silicon while varying the size until few nanometers, and loaded under mode I. The strain energy density is then defined as a function of the interatomic potential and averaged over the fracture process zone. Finally, by using an *attenuation function*, the atomic strain energy density gradient is *homogenized* to allow a comparison between the continuum and discrete formulation. Results show that the fracture process zone is scale independent, confirming that the ideal brittle fracture is ultimately governed by atomic bond-breaking. A singular stress field according to continuum fracture mechanics is still also present. However, when the singular stress field length (distance from the crack tip at which the stress deviates 5% from the theoretical field of $r^{0.5}$) is in the range of 4-5 times the fracture process zone, continuum fracture mechanics fails to describe the fracture, i.e., the breakdown of continuum theory. The new formulation, instead, goes well beyond that limit.

Keywords: atomistic simulation; multiscale; fracture mechanics; silicon; discrete fracture nanomechanics; strain energy density; nanoscale; brittle;

1. Introduction

Technological advancements in the fabrication of nanodevices (e.g., micro-nano electro-mechanical systems) have brought classic design issues addressed by continuum fracture mechanics into an entirely new field of applications. At such small scale, scientifically fundamental and practically critical questions arise on the validity of the classic fracture mechanics theory and its scale transition from macro to nano and, ultimately, to the atomic level. Extension of fracture mechanics to those small-scale components that are characterized by the very same problems encountered at the macroscale (e.g. presence of defects and stress raisers) is currently the next big challenge and a fundamental step for scientific advancements in nanotechnology.

The brittle fracture is an explicit situation where mechanical properties at the macroscale are characterized by events at the atomic level, i.e., the crack advances by atomic bond breaking. The first interpretation of this atomistic view of fracture can be dated back early this century, in the pioneering work of Griffith [1] who theorized that work must be done against the cohesive forces of atoms to generate material separation. The cohesive force to separate the bonds was then supposed to be dependent on interatomic force-displacement relationships, i.e., interatomic potential, and later associated with the surface energy per unit area. However, it has been only recently that those concepts have been addressed systematically, due to important advancements of in-situ observation of mechanical behavior at small scales [2–11] and developments of computational techniques such as molecular dynamics supported by improvement in computational power [12–14]. Sumigawa et al. [15] showed that the concept of "stress," clearly based on continuum assumptions, is still applicable to the fracture of samples approaching the nanoscale. Singular stress field of several nanometers, indeed, still control the fracture [16]. Intriguing, recent promising results in characterizing fracture at the atomic scale have been obtained by extending the Griffith criterion [17]. Huang et al. [18] considered notched components made of Silicon, and not only quantified a critical dimensional limit but proposed a unified Griffith-based criterion for both non-cracked and cracked systems.

Attempts to extend well-known linear elastic fracture mechanics concepts other than Griffith criterion to small scales have been made by several additional researchers [19–21] but within the limit of continuum formulation. These works certainly proved that, if the low limit of continuum fracture mechanics is not reached, classic linear elastic concepts can be extended to small scale, considering that some parameters may become size-dependent and should be evaluated accordingly. However, questions remain, for example, on how to precisely determine the low limit of continuum theory and how to consider the discrete nature of the system once beyond that limit [22,23]. Some attempts to include the effect of atoms discreteness have been made in the past [24,25]. Pugno and Ruoff, for example, proposed the so-called quantized fracture mechanics (QFM) [26]. The approach was energy based and substituted the differentials in Griffith's criterion with finite differences. However, the QFM also fails to describe the fracture below a critical specimen size. This result has been shown by Shimada et al. [27], who conducted a systematic investigation based on sophisticated numerical experiments on the breakdown of continuum theory and proposed an atomic-scale independent formulation of the energy release rate.

Based on the idea that energy concept is universal throughout all the material scales involved in the fracture process [28], we here proposed a unified strain energy density approach for brittle fracture that is valid from the atomic to the macroscale by considering the discrete nature of the strain energy density gradient in a body made of atoms. The paper summarized a series of numerical experiments based on molecular-statistics (MS) simulations of cracked samples by varying the size down to a few nanometers and loaded under mode I. The strain energy density is defined as a function of the interatomic potential, *homogenized* through an *attenuation function*, and averaged over the fracture process zone. The approach is finally compared with continuum formulation, which fails to describe fracture below a critical size. Finally, the breakdown of the continuum theory is evaluated and extensively discussed. The assumption of potential energy concept to characterize and describe material failure can be dated back to Huber, Freudenthal, and Hill [28,29] and early developments of the strain energy density concepts are summarized by Li [30]. The idea

to average the SED over a given control volume, instead, is mainly due to Lazzarin and co-workers [31–33]. Averaged strain energy density concept has been proved to be very flexible at the macroscale, and able to characterize static and fatigue behaviour of components under different loading conditions and with different geometrical features. Its extension in the frame of a discrete fracture mechanics theory would surely provide numerous advantages.

2. Method

2.1 Molecular statistics simulations, geometries, and mechanical properties

The fracture tests are conducted on nanoscale single-edge cracked specimens of brittle material *in silico* using molecular statistics (MS) simulations performed by using the open-source code LAMMPS [34]. By reference to Fig. 1, specimens of different sizes have been realized. The width W has been varied from 198.41 nm down to 9.81 nm and the crack length a is kept equal to $W/3$. In order to assure that there is no influence of the boundary conditions, the total height of the specimen is fixed to $2W$. The specimens are, therefore, "scaled" down by keeping constant their geometrical ratios.

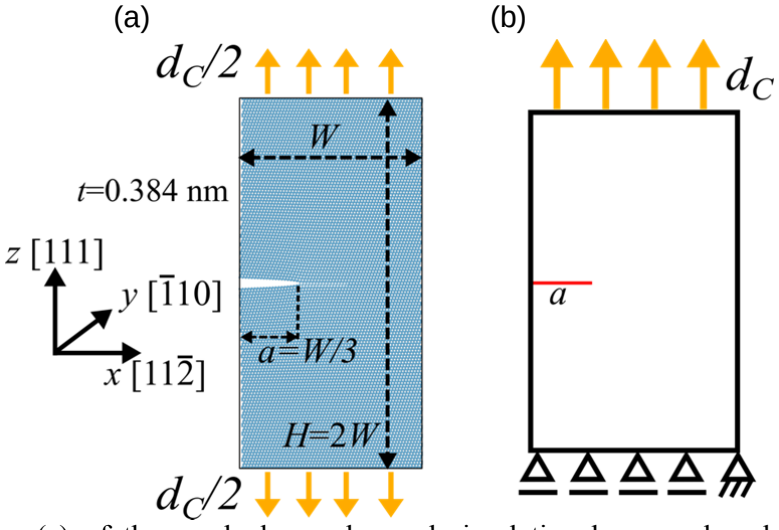

Fig. 1. Schematics (a) of the cracked samples and simulation box employed in the molecular statistics fracture tests (visualized through OVITO [35]), orientation, and (b) constraints configuration of FE model with critical displacement; t is the thickness of the simulation cell; the crack is slightly open to facilitate visualization.

The well-known modified Stillinger-Weber (SW) interatomic potential [36–38], widely used in the investigation of ideal brittle fracture *in silico*, is employed in the simulations. The samples have, therefore, the face-centered diamond-cubic structure of single crystal silicon and are oriented as depicted in Fig. 1a. The crack plane coincides with the cleavage plane (111), and it is perpendicular to the direction [111]. The mechanical properties and the lattice constant generated by the SW potential are reported in Table 1, together with the ideal material strength σ_{IS} = 35.2 GPa, i.e., the strength of a material ideally defect-free, along the direction [111]. This value has been estimated directly by the MS simulations of an un-cracked specimen, as shown in Fig. 3, that also depicts Young's modulus E_{111} of 209 GPa in the same direction. These values are also confirmed by other authors [18,39].

Table 1. The lattice constant, material constants, and mechanical properties obtained from the modified Stillinger-Weber potential.

Lattice constant (Å)	C_{11}(GPa)	C_{12} (GPa)	C_{44} (GPa)	E_{111} (GPa)	σ_{IS} (GPa)
5.431	201	51.4	90.5	209	35.2

A stepwise increment of strain ε is applied at the upper and lower layers of atoms of the specimens, as shown in Fig. 1a. The strain is increased at each load-step until the maximum displacement before final fracture d_C is reached, i.e. d_C is the critical displacement (at the critical load) before instant propagation of the crack occurs. Periodic boundary conditions are applied along the z-direction to replicate a plane-strain state. Periodic boundary, indeed, should approximate an infinite system by modeling only a part of it, i.e., the simulation box. Therefore, the simulation box has a finite thickness t in the z-direction of approximately 0.384 nm but if an atom passes through one side of the cell, it re-appears on the opposite side with the same velocity. At the beginning of the simulation and each strain/load increment, relaxation is ensured by using the damped dynamics method Fast Intertial Relaxation Engine (FIRE) [40] until all forces on atoms become less than $1.0 \bullet 10^{-5}$ μN.

The creation of a traction-free crack is realized by the so-called *screening* method: interactions between atoms on pre-crack surfaces are artificially deleted. Creation of traction free atomically sharp cracks can be somehow problematic when dealing with atomic systems because of the long-range interaction between atoms. A detailed discussion of crack modeling is out of the scope of the current work, but these problems and possible solutions are addressed by Andric et al. [13].

2.2 Finite Element Analyses

The fracture tests briefly introduced in section 2.1 are re-analyzed through Finite Element analyses. Single-edge cracked samples were modeled by using the *Ansys APDL 15.0* finite element software package. A 2D 8-node element-type PLANE183 [41] and plane strain conditions were assumed. For further accuracy, "concentration keypoint" was assumed to model the crack tip [41], and an accurate mesh was realized, with elements close to the crack tip approximately smaller than $a/10^5$. The concentration keypoint defines a point about which an area mesh will be skewed, and it is particularly useful for modeling stress concentrations and crack tips. The liner elastic anisotropic material model was selected. The stiffness matrix is derived from the three material constants of Table 1, i.e., C_{11}=201 GPa, C_{12}=51.4 GPa, C_{44}=90.5 GPa, for an orientation identical to that of atomistic simulations (see Fig. 1). The constraints configuration of the model is shown in Fig. 1b. Critical displacement d_C (maximum displacement at critical load, before crack propagation) obtained from MS simulations is then applied in order to evaluate stresses and other quantities at the critical condition under continuum mechanics theory.

3. Formulation of the discrete averaged strain energy density

The formulation of the discrete averaged strain energy density approach $aSED_{DFM}$ is a direct extension of the well-known averaged SED approach proposed in the past by Lazzarin and co-workers [31–33,42] at the macroscale. The approach reformulated here assumes that failure occurs

when the strain energy density averaged over a given control volume reaches a critical value W_C, and it is based on three key steps:

- The definition of the critical strain energy density at failure, W_C;
- The assumption of the control volume/area over which the discrete strain energy density is averaged;
- The definition of strain energy density as a function of the interatomic potential (*discrete formulation*).

Elastic deformations at the macroscopic level can be considered as a mutual behavior of atomic displacements from their equilibrium positions. This definition is particularly true for ideal brittle materials, (e.g., Silicon), where the atomic bond breaking governs the fracture, regardless of the specimen size [19,20,25]. Therefore, it is reasonable to assume that the discrete critical strain energy density has a similar formulation of its macroscale/continuum counterpart [43], provided that the correct mechanical properties are employed. This assumption is particularly convenient in the case of the SW potential used in the present study. The material behavior is indeed orthotropic, defined by the three material constants reported in Table 1 or, eventually, by an equivalent isotropic behavior for in-plane loadings. For these reasons, the critical strain energy density at failure W_C of the samples under considerations in the present paper, under mode I loading, is a direct extension of the critical SED as derived in [31,33,43] for macroscale isotropic continuum component, and reduces to the following form:

$$W_C = \frac{\sigma_{IS}^2}{2E_{111}} \ , \tag{1}$$

where σ_{IS} is the ideal material strength, E_{111} is Young's modulus along the direction [111]. Both quantities are derived from MS simulation of an un-cracked sample (see Table 1 or Fig. 3 of the results, section 4.1).

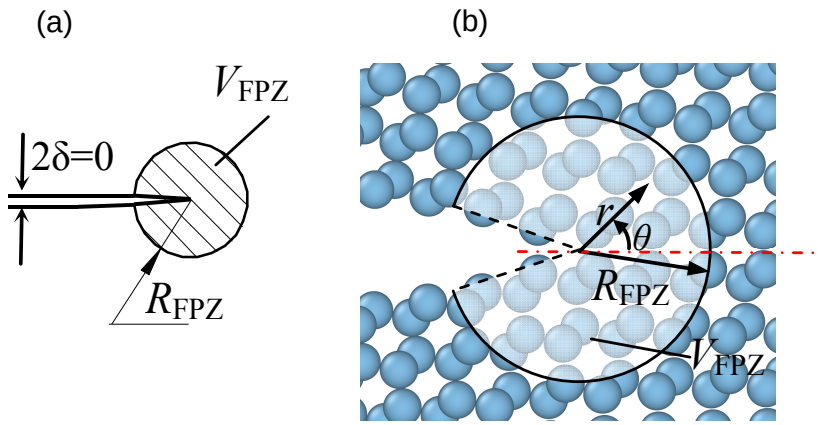

Fig. 2. Schematics of the (a) control volume in classic continuum body in the case of a crack under mode I loading, and (b) in the atomic model; r is the generic distance from crack tip in cylindrical coordinates, R_{FPZ} and V_{FPZ} are the radius and volume, respectively, of the fracture process zone; the crack in (b) is slightly open to facilitate visualization.

Concerning Fig. 2**,** the so-called fracture process zone (FPZ), defined as the zone where nonlinear phenomena appear and the discrete motion of atoms is highly concentrated, is assumed as the control volume V_{FPZ}. The FPZ is considered to be the material characteristic zone that controls the fracture in the case of ideal brittle materials [27,44]. For simplicity, in the case of a crack under mode I loading, it is described by a radius R_{FPZ} centered at the crack tip, and its length is determined later by analyzing the atomic SED distribution in the results section 4.1. The volume V_{FPZ} is therefore merely $(\pi R_{FPZ}^2)t$. The crack tip in the discrete body is hypothetically positioned between the atoms at the beginning of the crack plane, as shown in Fig. 2b.

Lazzarin and Berto [31,43], as well as several other authors [45–47] showed that in the case of sharp V-notches the control area becomes a circular sector, while in the case of blunt notches the area assumes a crescent shape and it is centred at distance "r_0" from the notch root. In case of mixed mode, the control volume is no longer centred with respect to the notch bisector, but rigidly rotated with respect to it and centred on the point where the SED reaches its maximum value. Since the present work focuses preliminarily only on cracks under mode I loading, those cases are not reported here, but details are available in the given references. Let us just emphasize how the

literature on the aSED is vast, and demonstrates the flexibility of the method in assessing both static and fatigue behaviour of components of different geometries and loading conditions.

The discrete formulation of the averaged strain energy density $aSED_{DFM}$ is evaluated as the sum of the SED of all the atoms included in the FPZ divided by V_{FPZ}:

$$aSED_{DFM} = \frac{\sum_{V_{FPZ}} SED_{ATOM}}{V_{FPZ}} \ . \tag{2}$$

For a given generic atom i at a distance r from the crack tip, its $SED_{ATOM\ i}$ is defined as the difference between the atomic potential energy at the critical displacement d_C and the unloaded condition, multiplied by an *attenuation function* $\alpha(r_i)$ [48], as follows:

$$SED_{ATOM\ i} = \left[\Pi_{ATOM\ i}(d_C) - \Pi_{ATOM\ i}(o)\right] \cdot \alpha(r_i) = \Delta\Pi_i \cdot \alpha(r_i) \tag{3}$$

The attenuation function depends on the distance r between the atoms and crack tip, and it is defined by the following equation:

$$\alpha(r) = c\left\langle 1 - \frac{r^2}{R_{FPZ}^2} \right\rangle^2 \tag{4}$$

where c is the scaling factor, R_{FPZ} is the radius of the fracture process zone while the Macauley brackets $\langle \ldots \rangle$ denote the positive part, i.e. $\langle x \rangle = \max(0,x)$. The attenuation function, taken from theory of non-local elasticity [49], states that interaction effects decay with distance between two points over the interaction radius R_{FPZ}, i.e. when $r >> R_{FPZ}$ the atoms do not provide any contribution to the SED averaged over the FPZ, while contribution of atoms inside the FPZ is "scaled" accordingly to their distance from the crack tip. Simplifying, the employment of the attenuation function is nothing but *homogenization* of the SED gradient that would be heterogeneous and discrete because of the discrete nature of atoms. This process brings enormous advantages since it permits to easily assume a possible exact crack tip position (it is itself not exact in a body made of atoms) and to treat atoms that, being on the border of the control volume, would have a small and undefined contribution to the fracture process zone. The homogenization through the attenuation function is a fundamental step to enable a comparison with continuum counterpart. An extensive discussion on all these

aspects, needs and implications of using the attenuation function is presented in the Supplementary Material S.2. Lastly, the scaling factor c is here determined by equating the $aSED_{DFM}$ and W_C, i.e.:

$$c = \frac{W_C \cdot V_{FPZ}}{\sum_{V_{FPZ}} \left\{ \left[\Pi_{ATOM\,i}(d_C) - \Pi_{ATOM\,i}(o) \right] \cdot \left\langle 1 - \frac{r_i^2}{R_{FPZ}^2} \right\rangle^2 \right\}} \tag{5}$$

If one sample is assumed as a reference, and the FPZ is known, all the variables in the right term of the Equation (5) are known too. It is anticipated that the sample W=150.77 nm (and only that) is used to calibrate the scaling factor; determined value is later kept constant for all the geometries. Physical meaning and theoretical developments of the scaling factor are possible but left for future work, while further comments are provided in the given references. The results will soon show a fracture process zone of approximately 0.4 nm (average value) and a corresponding scaling factor of 2.252.

4. Results and discussion

4.1 SED gradient and fracture process zone

Figure 3 shows the global σ-ε curve of an un-cracked specimen and the SW potential mechanical properties along the direction [111]. The ideal material strength σ_{IS} is approximately 35.2 GPa, while Young's modulus E_{111} is 209 GPa. These are traditional values when the SW potential is employed [18]. By using Eq. (1) and the mechanical properties just evaluated, it results in a critical strain energy density value W_C=2.962 GJ/m^3. Figure 4 shows, instead, global σ-ε curves of cracked samples and relative critical displacement d_C at failure. The figure presents only the results of the samples W=19.87 nm, 51.78 nm, and 150.77 nm to make the graph clearer; all the other values are presented in the Table S.1 (Supplementary Material). The picture demonstrates that the samples, regardless of their size, show a linear behavior until final failure. The deformation is globally always under linear elastic condition, without any plastic phenomena involved, e.g., dislocations. At a critical load, the crack propagates instantly and results in the specimen failure. These observations support the idea that the fracture is ultimately governed by the breaking of an atomic bond at the

crack tip. The critical displacement d_C is therefore defined as the displacement at the critical load, just before crack propagation and final failure take place.

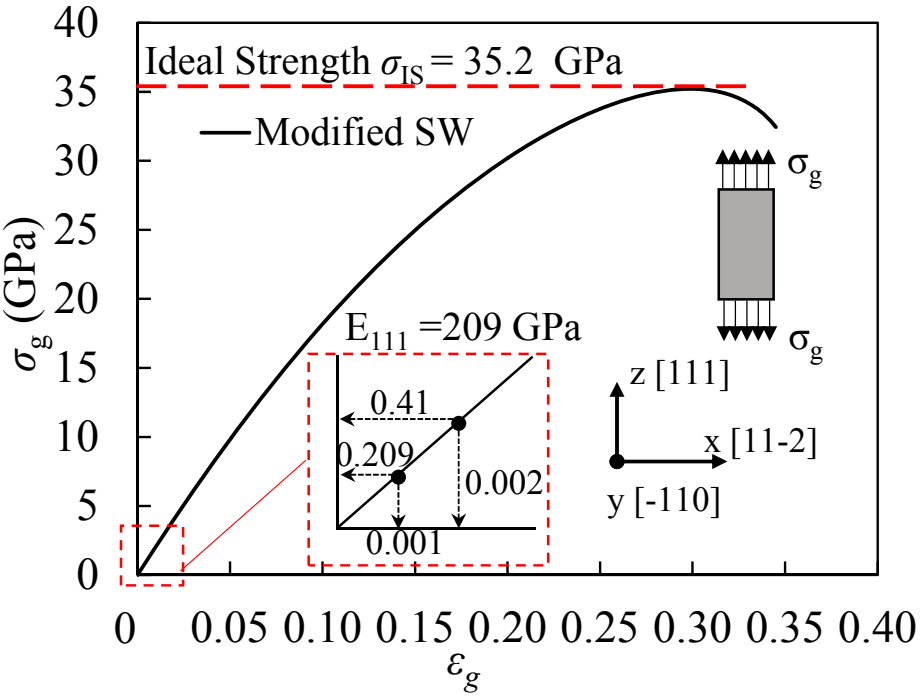

Fig. 3. Global σ-ε curve of un-cracked specimens obtained from MS numerical experiments, and mechanical properties along the direction [111]; specimen width W=100 nm.

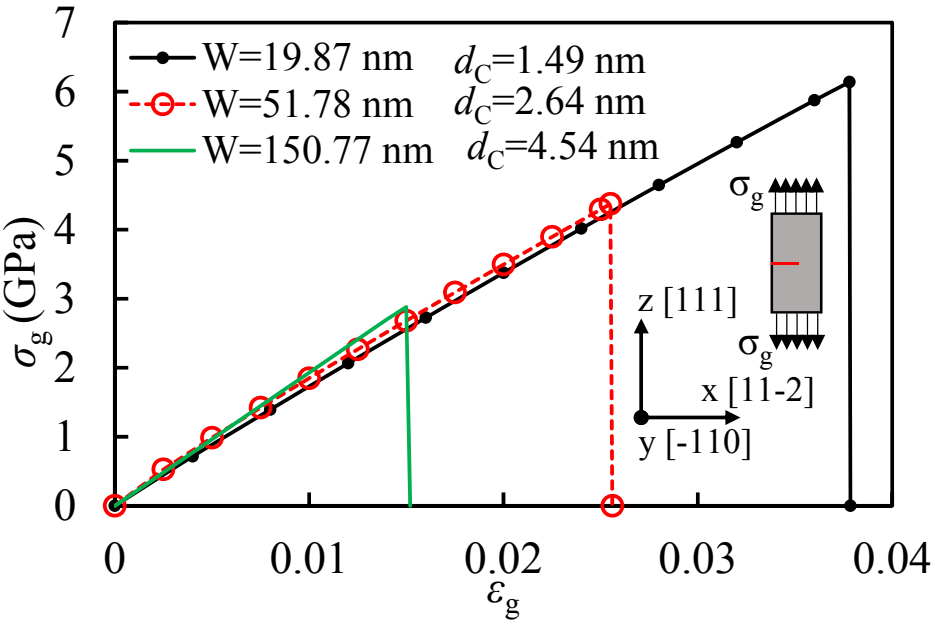

Fig. 4. Global σ-ε curve of selected single-edge cracked specimens obtained from MS numerical experiments and critical displacement d_C (i.e. maximum displacement at the critical load).

The strain energy density distribution at the crack tip was also analyzed to determine the fracture process zone, defined as the *distance from crack tip where the SED contribution is concentrated*. Fig. 5 depicts a graphical representation of the gradient at the crack tip in the atomic body, while Fig. 6 shows the main results. For the sake of clarity, it should be noted that this SED is evaluated as a simple difference between the interatomic potential energy of the sample at the critical displacement d_C and unloaded model for each atom, i.e., it is not averaged and it is not processed through the attenuation function. It is therefore labeled in Fig. 6 as $\Delta\Pi$ to avoid misunderstanding. The graphical representation in Fig. 5 shows a clear circular zone where the SED is highly localized. The picture compares W=19.87 nm and W=150.77 nm. However, same results have been obtained for all the other geometries: regardless of the specimen size, this zone has an identical dimension in the range of 0.35-0.45 nm (≈ 1-1.5 atomic distance along the crack plane), in average 0.4 nm, and it is representative of the fracture process zone. This value is in the expected range (~ nm) of ideal brittle material as suggested by Pippan et al. [44] and Shimada et al. [27]. This conclusion is further confirmed by Fig. 6 that depicts the values of the SED distribution at the crack tip by considering only upper atoms along the crack plane, normalized by the SED at the crack tip atom, where the maximum value is found. The primary contribution to the SED is given by the atoms at the crack tip and concentrated in a distance of approximately 0.35-0.45 nm; at 0.8 nm, $\Delta\Pi/\Delta\Pi_{max}$ decreases to 0.1, making any other contribution at greater distances (but in the proximity of the crack tip) negligible when averaging over the volume. Same results and precisely the same trend are found for all the other specimens: again, it is confirmed that the atoms involved in the fracture process are the same, regardless of the considered size, and are localized around the crack tip in a distance of approximately 0.4 nm (average value). From these considerations, the FPZ (i.e. distance from crack tip where the SED contribution is concentrated) is assumed to be 0.4 nm in the subsequent evaluation of the $aSED_{DFM}$. By considering the finite thickness t of the simulation cell (see Fig. 1 and section 2.1), the control volume V_{FPZ} is then $(\pi R_{FPZ}^2)t = 0.193\ \text{nm}^3$. Supplementary

Material (see S.2) further confirms a size of the fracture process zone of 0.4 nm (as average value) by considering, alternatively, the non-linear behaviour of the approximated derivative of the aSED values over the variation of the control volume. Regarding atomic motions of Fig. 5 and Fig. 6, it should be noted that despite the severe localized crystallographic distortion of the FPZ, phenomena such as atomic reconstruction, surface reconstruction or phase transformation did not occur. The interatomic bond is simply broken as the crack nucleates and propagates, and the at the crack-tip area (i.e., the FPZ), the original diamond structure of Si atoms is kept even before and during fracture process. These results have been further demonstrated by Shimada et al. [27] who employed exactly the same interatomic potential used in the present study and observed fracture process precisely. The fracture in the present work is thus ideally brittle.

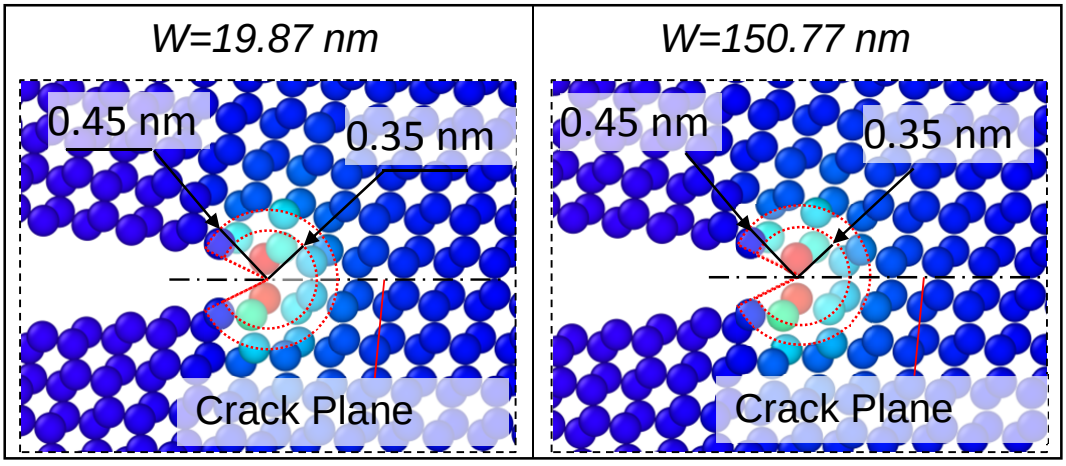

Fig. 5. Atomic SED distribution at the crack tip for different sample widths *W*; the SED is here evaluated atom by atom as difference of interatomic potential at the critical displacement and unloaded model (i.e. ΔΠ is not averaged and not processed through the attenuation function); the fracture process zone is in the range of 0.35-0.45 nm, 0.4 nm in average; visualized in OVITO [35].

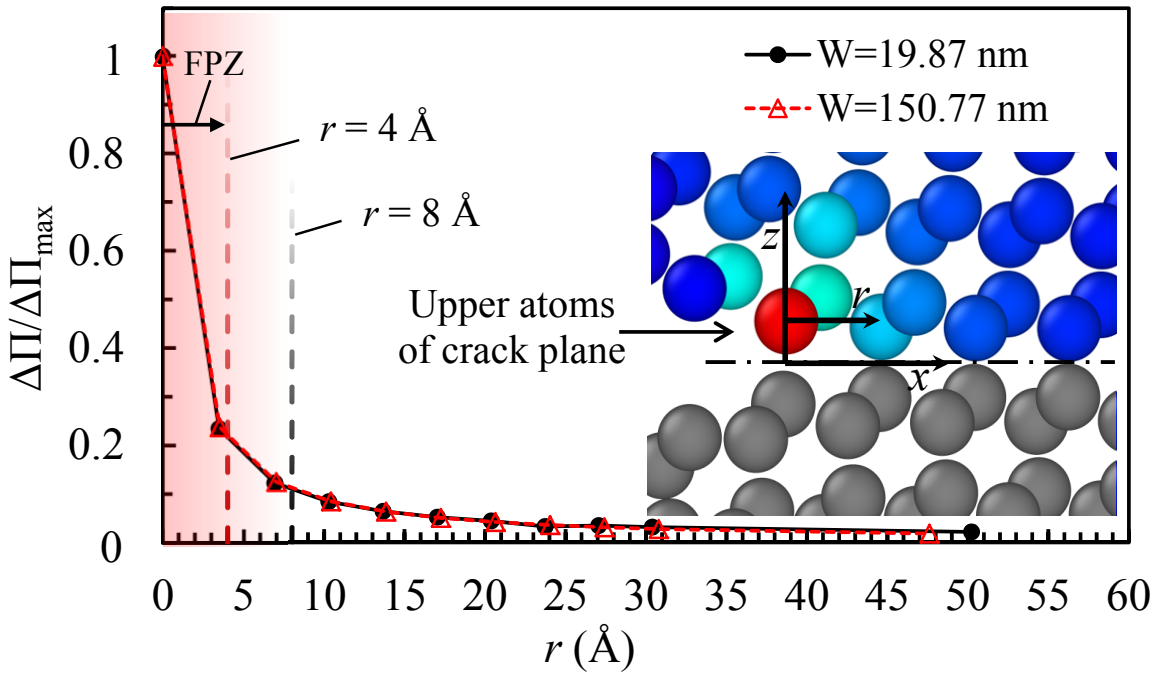

Fig. 6. Atomic SED distribution for the upper atoms of the crack plane normalized by the maximum value; the SED is not attenuated and not averaged (i.e. simple difference of atomic potentials, ΔΠ); the maximum value is found for the atom at the crack tip (r=0).

Having defined the FPZ and the W_C, the $aSED_{DFM}$ can be finally quantified according to Eq. (2) and compared with FE analyses. The results are shown in Fig. 7. The scaling factor c=2.252 of the attenuation function is calibrated according to Eq. (5) by using only the MS results of the specimen W=150.77 nm and it is kept constant for all the other geometries. For the sake of clarity, the steps for the calculation of the $aSED_{DFM}$ are briefly re-called: (i) the SED of each atom is defined as difference of its potential energy at the critical displacement d_C and unloaded configuration; (ii) each value is then multiplied by the attenuation function, i.e. *homogenization* of the SED gradient over the FPZ; (iii) the contributions are finally summed together and averaged over the FPZ. The results clearly show that the $aSED_{DFM}$ at critical condition is constant, regardless of the specimen width, and it is in excellent agreement with the theoretical critical value W_C of Eq. (1). A small variation of ± 3% is to be expected, because of the finite step increment of strain in the MS simulations and the keen sensitivity of the SED to the displacement values as such small scales. By superimposing the results from continuum analyses, a good agreement within the range of ±3% is

found for very large samples: the SED at fracture is constant, in agreement with the discrete formulation and the critical theoretical value. However, at a width of approximately 40-50 nm, the LEFM starts to deviate from the expected results, i.e. breakdown of continuum theory. The deviation, that underestimates the critical SED at fracture, increases as the specimens become smaller. By considering the sample of width W=9.87 nm, it gives a critical SED of 2.344 GJ/m^3, that is 27% smaller than the expected value of 2.962 GJ/m^3. The next section 4.2 will further address the breakdown of continuum theory, and provide a more general definition based on the length of the fracture process zone (from MS numerical experiments) and the length of the singular stress field (from LEFM).

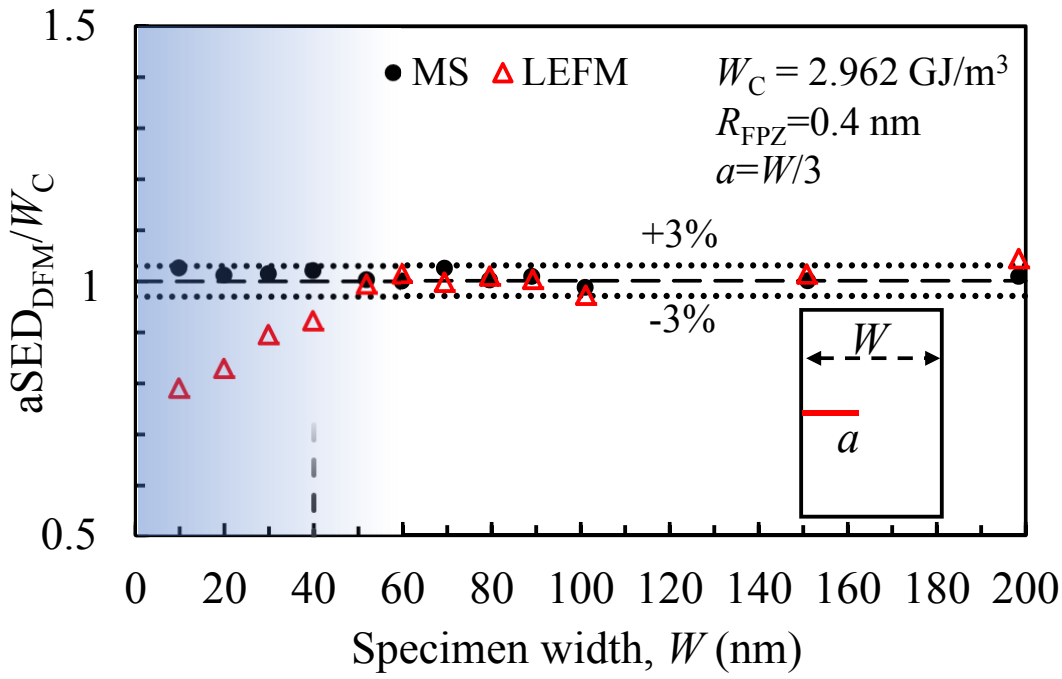

Fig. 7. Comparison between aSED based on the discrete fracture mechanics formulation (MS simulations) and LEFM, as a function of the specimen width; the values are normalized by the theoretical critical SED at fracture of Eq. (1).

4.2 Breakdown of continuum theory

The results summarized in Fig. 7 demonstrates that the new discrete fracture mechanics formulation of the strain energy density is more general than its continuum counterpart. Indeed, aSED$_{DFM}$ has an

excellent agreement with the critical theoretical value regardless of the specimen size, while continuum formulation fails below a width W of 40-50 nm. However, a more general definition of the length scale beyond which the continuum formulations fails can be provided by analyzing the length of the FPZ (evaluated from MS results), and the *K-dominated zone* Λ_K (from LEFM analyses) defined as the distance from the crack tip at which the stresses deviate 5% from the theoretical $r^{0.5}$ field. It is shown in Figure 8(b) that the largest specimen has a Λ_K of approximately 7.78 nm, a quite significant value if compared to the FPZ of 0.4 nm. However, for the small sample in Fig. 8(a), the length of Λ_K decreases to only 0.42 nm, very close to the FPZ size. In other words, when reducing the samples widths, K-dominated zone Λ_K shrinks down, while the FPZ remains constant. At a critical length, the primary assumption of the LEFM formulation $R_{FPZ}<<\Lambda_K$ is not satisfied anymore. This aspect is highlighted in Fig. 9 that permits to quantify the ratio between Λ_K and the FPZ at which the LEFM deviates from MS results. When the singular stress field is in the range of 4 to 5 times the FPZ (W=40-50 nm), i.e. 1.5-2 nm, continuum fracture mechanics fails. Similar results have been recently confirmed by Shimada et al. [27] who employed sophisticated numerical experiments on pre-cracked nanoscale specimens. Those authors estimated a fracture process zone of approximately 0.4-0.6 nm, and a low limit of continuum fracture mechanics in the range of 3-6 the FPZ. As long as the non-linear behavior is well confined in a FPZ very small in comparison to the K-dominated region, classic LEFM still valid. This conclusion justifies why several authors have successfully applied classic concepts to small scales [15,16,50–52].

Considerations and analyses on stress intensity factors and fracture toughness have been intentionally ignored to focus on the energy concepts only. However, it should be noted that W_C can characterize the fracture at different scales, i.e. it is scale-independent, and this results further confirmed that the fracture toughness of ideal brittle materials is fundamentally inherent [16,52].

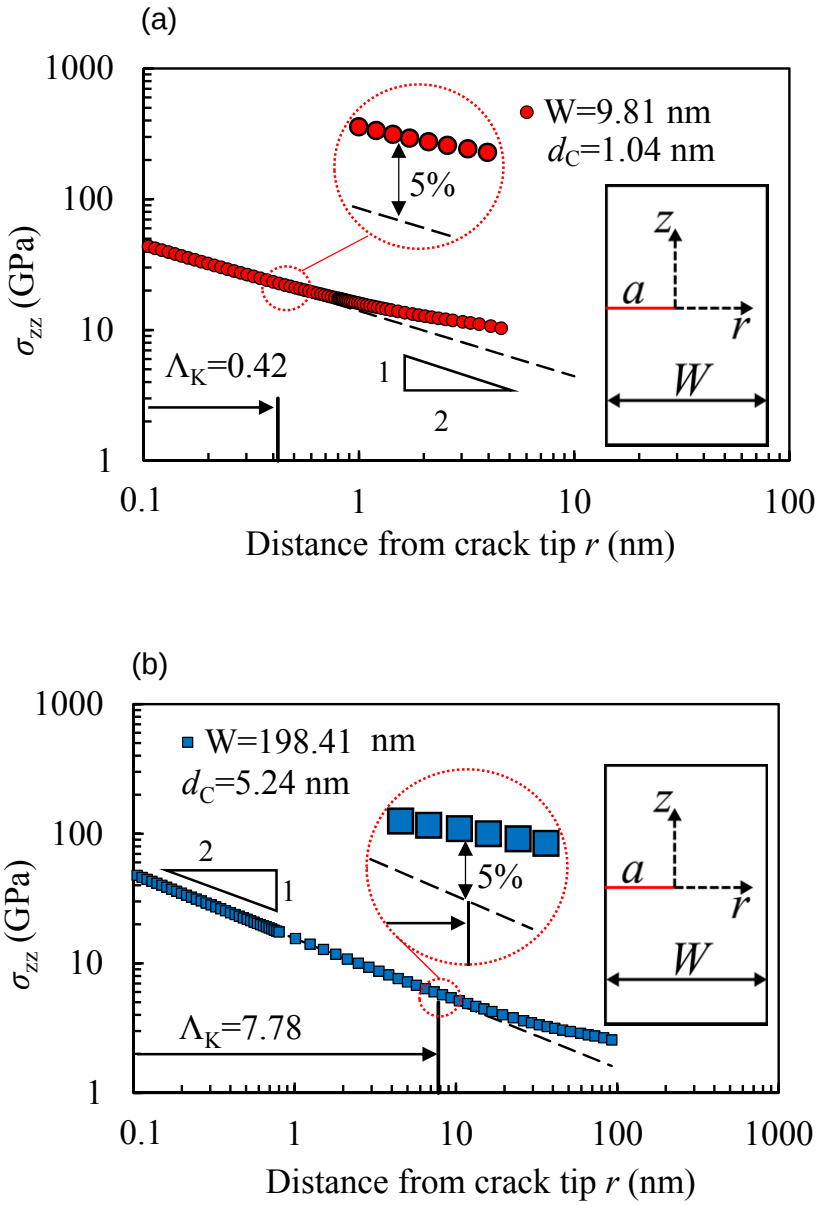

Fig. 8. Singular stress field lengths (K-dominated region) for specimens width (a) W=9.81 nm and (b) W=198.41 nm obtained from FE analyses; the singular stress field length is defined as the distance from the crack tip at which the stress deviates 5% from the theoretical field of $r^{0.5}$.

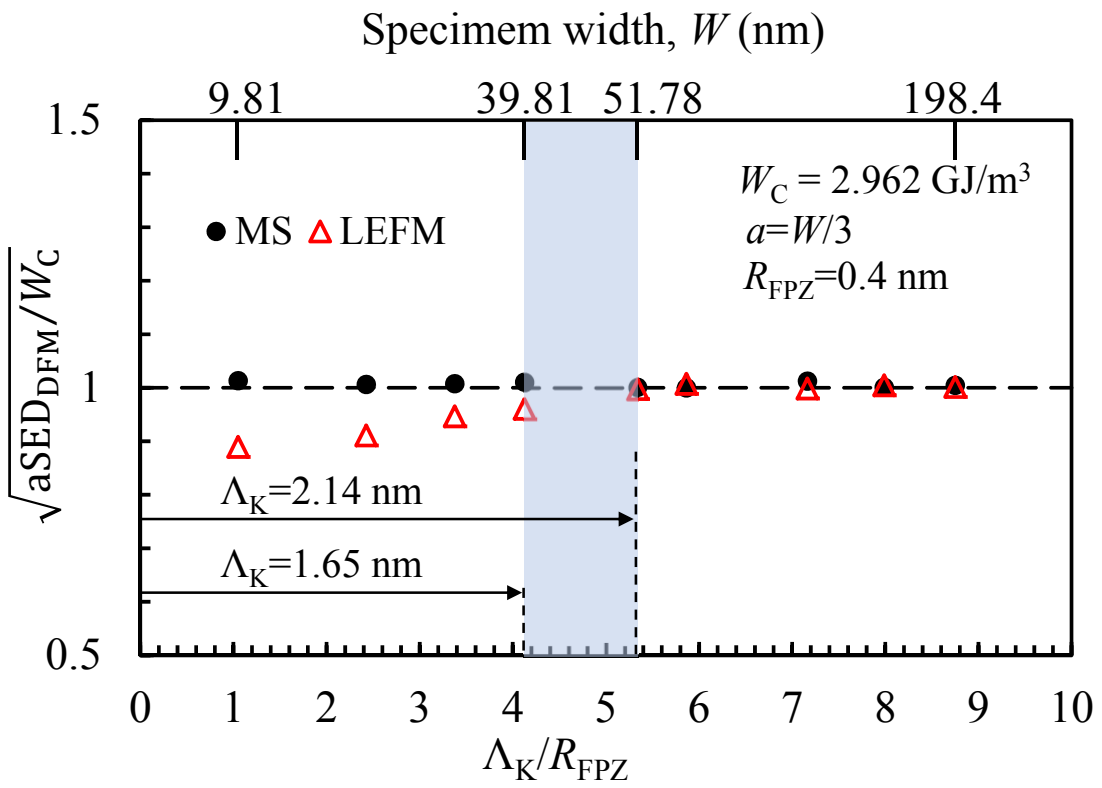

Fig. 9. Normalized fracture test results in terms of the ratio between the length of the K-dominated region Λ_K (from LEFM analyses), and the fracture process zone R_{FPZ} (evaluated from MS simulations).

4.3 Final remarks and future challenges

Classic LEFM works very well when dealing with bulk material, where the characteristic material length, e.g. the fracture process zone for brittle material, is confined in a very small zone. However, when the material becomes heterogenous or when the local microstructure cannot be ignored, a more physically based approach is needed. One way is to rely on models based on atomic interactions, as shown in the present work. Unfortunately, interatomic potentials are defined for limited systems, and even if the physic of the problem is correctly replicated, they tend to deviate from actual experimental results which are far from the ideal conditions. In other words, a critical strain energy density evaluated by atomic simulations may be different from experimental values already at the microscale. These aspects do not affect the validity of the method when investigating the physical processes involved but indeed represent a future challenge if the final aim is the

proposition of a universal approach that spans different materials and that correctly estimates actual experimental results.

The present work has considered ideal brittle fracture only, under monotonic mode I load. It is undoubted that the real big challenge is the fatigue phenomenon. In this regard, it will be crucial the evaluation of the scale at which mechanisms of fatigue occur and their scale transitions to finally propose a more general scale-independent formulation or to improve the current approaches. Atomic simulations and small-scale experiments can provide enormous contribution when investigating, for example, the role of dislocations, microstructure, and short-crack growth. When dealing with fatigue, it should be expected a different size of the fracture process zone, since the physical processes involved are different than those of ideal brittle fracture, and occur at a different scale level [44].

Concluding, the study was limited to the characterization of cracked components under mode I loading since the main target was a preliminary investigation of the breakdown of continuum theory based on a reformulated discrete SED approach. Extension of the approach to other loading conditions and notches is undoubtedly intriguing but left for future work. In cracked components, fracture occurs obviously by atomic bond breaking at the crack tip. However, in the case of large notches, authors have found some difficulties to identify *a priori* the proper atomic bond at which the fracture would occur and to correctly place the small control volume. Indeed, according to [33,43] and to section 3 briefly, in the case of blunt notches the area of the control volume assumes a crescent shape and it is centred at distance "r_0" from the notch root; in case of mixed mode, the control volume is rigidly rotated and centred on the point where the SED reaches its maximum value. These definitions imply the implicit knowledge or assumption of the location of the crack initiation, and place the control volume accordingly.

Finally, the definition of the critical SED in Eq. (1) has been provided by considering a crack along the cleavage plane (111) and the Young's modulus accordingly, i.e. in its scalar form. A more general formulation would necessarily involve a full consideration of the anisotropic behaviour, and

it is left for future work. Success in this direction would provide a method that is both scale- and potentially (based on results at the macroscale) geometric independent, i.e., it would characterize successfully notches and cracks at any scale, while remaining very simple. Geometric independency is, indeed, the main advantage when employing the classic aSED formulation at the macroscale (see e.g. [43]).

5. Conclusions

The present work investigated the ideal brittle fracture at macro- to nano- (even atomic) scales, and proposed a new formulation of the averaged strain energy density based on discrete fracture mechanics theory, namely $aSED_{DFM}$. The strain energy density was defined as a function of the interatomic potential, *homogenized* through an *attenuation function*, and averaged over the fracture process zone. A series of numerical experiments based on MS simulations on ideal brittle fracture *in silico* under mode I loading were realized to support and verify the formulation. The approach was finally compared with continuum fracture mechanics theory. The main conclusions can be summarized as follows:

- The proposed formulation of the $aSED_{DFM}$ is scale independent, and correctly characterize the fracture from the macro to the nanoscale under mode I loading condition;
- Continuum-based formulation of the aSED fails to describe the fracture below a critical size;
- The critical K-dominated length at which continuum formulation fails, i.e. breakdown of continuum theory, is found to be in the range of 4-5 times the fracture process zone;
- A singular stress field of just a few nanometers in agreement with classic LEFM formulation is still present even for the smallest specimens;
- The ideal brittle fracture is governed by atomic bond breaking at the crack tip since the fracture process zone is constant (scale independent) and approximately in the range of 0.35-0.45 nm (based on SED gradient), regardless of the specimen size;

- It is demonstrated that, if the discrete nature of atoms is considered, the critical strain energy density at fracture is constant and scale independent, thus fracture toughness is fundamentally inherent as verified by other authors [27,52].
- The work is limited, preliminarily, to mode I loading of cracked components; however, the vast literature on the classic aSED concept has demonstrated a high degree of validity by assessing both static and fatigue behaviour of components of different geometries, under different loading conditions and made of different materials. As a future work, further investigation of those additional cases should be performed, as well as additional orientations of the samples should be considered.

Acknowledgments

This work was supported by the Japan Society for the Promotion of Science (JSPS) (Grant-in-Aid for JSPS Fellows No.16F16366, KAKENHI 18H05241, 18K18806 and 17H03145), Academy of Finland (project number 298762 mFAT, 310828 StrainPath).

P.G. wrote the paper and is the main contributor of the proposed ideas; Y.H. realized part of the MS simulations; T.S. gave valuable support on the realization of the MS simulations and their discussion; T.K. revised the work and gave valuable comments on the manuscript. The first author is grateful to Prof. J. Romanoff and H. Remes (Aalto University).

Bibliography

[1] A.A. Griffith, The phenomena of rupture and flow in solids, Philos. Trans. R. Soc. London. 221 (1921) 163–198.

[2] T. Sumigawa, T. Kitamura, In-Situ Mechanical Testing of Nano-Component in TEM, in: K. Maaz (Ed.), Transm. Electron Microsc., InTech, 2012: pp. 355–380.

[3] D.S. Gianola, A. Sedlmayr, R. Mönig, C.A. Volkert, R.C. Major, E. Cyrankowski, S.A.S. Asif, O.L. Warren, O. Kraft, In situ nanomechanical testing in focused ion beam and scanning electron microscopes, Rev. Sci. Instrum. 82 (2011) 063901. doi:10.1063/1.3595423.

[4] M.J. Pfeifenberger, M. Mangang, S. Wurster, J. Reiser, A. Hohenwarter, W. Pfleging, D. Kiener, R. Pippan, The use of femtosecond laser ablation as a novel tool for rapid micro-mechanical sample preparation, Mater. Des. 121 (2017) 109–118. doi:10.1016/j.matdes.2017.02.012.

[5] T. Kitamura, T. Sumigawa, H. Hirakata, T. Shimada, Fracture Nanomechanics, 2nd ed., Pan Stanford Publishing, Singapore, 2016.

[6] Y. Yan, T. Sumigawa, T. Kitamura, A Robust in situ TEM Experiment for Characterizing the Fracture Toughness of the Interface in Nanoscale Multilayers, Exp. Mech. 58 (2018) 721–731. doi:10.1007/s11340-018-0375-6.

[7] J. Ast, M. Ghidelli, K. Durst, M. Goeken, M. Sebastiani, A.M. Korsunsky, A review of experimental approaches to fracture toughness evaluation at the micro-scale, Mater. Des. (2019) In Press. doi:10.1016/j.matdes.2019.107762.

[8] F.Y. Cui, R.P. Vinci, A chevron-notched bowtie micro-beam bend test for fracture toughness measurement of brittle materials, Scr. Mater. 132 (2017) 53–57. doi:10.1016/j.scriptamat.2017.01.031.

[9] F. Iqbal, J. Ast, M. Göken, K. Durst, In situ micro-cantilever tests to study fracture properties of NiAl single crystals, Acta Mater. 60 (2012) 1193–1200. doi:10.1016/j.actamat.2011.10.060.

[10] D. Kupka, N. Huber, E.T. Lilleodden, A combined experimental-numerical approach for elasto-plastic fracture of individual grain boundaries, J. Mech. Phys. Solids. 64 (2014) 455–467. doi:10.1016/j.jmps.2013.12.004.

[11] P. Gallo, T. Sumigawa, T. Kitamura, Experimental characterization at nanoscale of single crystal silicon fracture toughness, Frat. Ed Integrità Strutt. 13 (2019) 408–415. doi:10.3221/IGF-ESIS.47.31.

[12] E. Bitzek, J.R. Kermode, P. Gumbsch, Atomistic aspects of fracture, Int. J. Fract. 191 (2015) 13–30. doi:10.1007/s10704-015-9988-2.

[13] P. Andric, W.A. Curtin, Atomistic modeling of fracture, Model. Simul. Mater. Sci. Eng. 27 (2018) 013001. doi:10.1088/1361-651x/aae40c.

[14] M. Mosby, K. Matouš, Computational homogenization at extreme scales, Extrem. Mech. Lett. 6 (2016) 68–74. doi:10.1016/j.eml.2015.12.009.

[15] T. Sumigawa, H. Fang, E. Kawai, T. Kitamura, Mechanics of fracture in nanometer-scale components, Mech. Eng. Rev. 1 (2014) SMM0007–SMM0007. doi:10.1299/mer.2014smm0007.

[16] T. Sumigawa, T. Shimada, S. Tanaka, H. Unno, N. Ozaki, S. Ashida, T. Kitamura, Griffith

Criterion for Nanoscale Stress Singularity in Brittle Silicon, ACS Nano. 11 (2017) 6271–6276. doi:10.1021/acsnano.7b02493.

[17] H. Yin, H.J. Qi, F. Fan, T. Zhu, B. Wang, Y. Wei, Griffith criterion for brittle fracture in graphene, Nano Lett. 15 (2015) 1918–1924. doi:10.1021/nl5047686.

[18] K. Huang, T. Shimada, N. Ozaki, Y. Hagiwara, T. Sumigawa, L. Guo, T. Kitamura, A unified and universal Griffith-based criterion for brittle fracture, Int. J. Solids Struct. 128 (2017) 67–72. doi:10.1016/j.ijsolstr.2017.08.018.

[19] P. Gallo, Y. Yan, T. Sumigawa, T. Kitamura, Fracture Behavior of Nanoscale Notched Silicon Beams Investigated by the Theory of Critical Distances, Adv. Theory Simulations. 1 (2018) 1700006. doi:10.1002/adts.201700006.

[20] P. Gallo, T. Sumigawa, T. Kitamura, F. Berto, Static assessment of nanoscale notched silicon beams using the averaged strain energy density method, Theor. Appl. Fract. Mech. 95 (2018) 261–269. doi:10.1016/j.tafmec.2018.03.007.

[21] P. Gallo, T. Sumigawa, T. Kitamura, F. Berto, Evaluation of the strain energy density control volume for a nanoscale singular stress field, Fatigue Fract. Eng. Mater. Struct. 39 (2016) 1557–1564. doi:10.1111/ffe.12468.

[22] T. Kitamura, T. Sumigawa, T. Shimada, L. Van Lich, Challenge toward nanometer scale fracture mechanics, Eng. Fract. Mech. 187 (2018) 33–44. doi:10.1016/j.engfracmech.2017.10.009.

[23] G. Dehm, B.N. Jaya, R. Raghavan, C. Kirchlechner, Overview on micro- and nanomechanical testing: New insights in interface plasticity and fracture at small length scales, Acta Mater. 142 (2018) 248–282. doi:10.1016/j.actamat.2017.06.019.

[24] E. Tarleton, D.S. Balint, J. Gong, A.J. Wilkinson, A discrete dislocation plasticity study of the micro-cantilever size effect, Acta Mater. 88 (2015) 271–282. doi:10.1016/j.actamat.2015.01.030.

[25] T. Shimada, T. Kitamura, Fracture Mechanics at Atomic Scales, in: H. Altenbach, T. Matsuda, D. Okumura (Eds.), Adv. Struct. Mater., Springer International Publishing, Cham, 2015: pp. 379–396. doi:10.1007/978-3-319-19440-0_17.

[26] N.M. Pugno, R.S. Ruoff, Quantized fracture mechanics, Philos. Mag. 84 (2004) 2829–2845. doi:10.1080/14786430412331280382.

[27] T. Shimada, K. Ouchi, Y. Chihara, T. Kitamura, Breakdown of Continuum Fracture Mechanics at the Nanoscale, Sci. Rep. 5 (2015) 8596. doi:10.1038/srep08596.

[28] A.M. Freudenthal, The Inelastic Behavior of Engineering Materials and Structures, John Wiley & Sons, New York, 1950.

[29] R. Hill, A variational principle of maximum plastic work in classical plasticity, Q. J. Mech. Appl. Math. 1 (1948) 18–28. doi:10.1093/qjmam/1.1.18.

[30] Q.M. Li, Strain energy density failure criterion, Int. J. Solids Struct. 38 (2001) 6997–7013. doi:10.1016/S0020-7683(01)00005-1.

[31] P. Lazzarin, R. Zambardi, A finite-volume-energy based approach to predict the static and fatigue behavior of components with sharp V-shaped notches, Int. J. Fract. 112 (2001) 275–298. doi:10.1023/A:1013595930617.

[32] P. Lazzarin, R. Zambardi, The Equivalent Strain Energy Density approach re-formulated and applied to sharp V-shaped notches under localized and generalized plasticity, Fatigue Fract. Eng. Mater. Struct. 25 (2002) 917–928. doi:10.1046/j.1460-2695.2002.00543.x.

[33] F. Berto, P. Lazzarin, A review of the volume-based strain energy density approach applied to V-notches and welded structures, Theor. Appl. Fract. Mech. 52 (2009) 183–194. doi:10.1016/j.tafmec.2009.10.001.

[34] S. Plimpton, Fast Parallel Algorithms for Short-Range Molecular Dynamics, J. Comput. Phys. 117 (1995) 1–19. doi:10.1006/jcph.1995.1039.

[35] A. Stukowski, Visualization and analysis of atomistic simulation data with OVITO–the Open Visualization Tool, Model. Simul. Mater. Sci. Eng. 18 (2010) 015012. doi:10.1088/0965-0393/18/1/015012.

[36] D. Holland, M. Marder, Ideal Brittle Fracture of Silicon Studied with Molecular Dynamics, Phys. Rev. Lett. 80 (1998) 746–749. doi:10.1103/PhysRevLett.80.746.

[37] D. Holland, M. Marder, Cracks and atoms, Adv. Mater. 11 (1999) 793–806. doi:10.1002/(SICI)1521-4095(199907)11:10<793::AID-ADMA793>3.0.CO;2-B.

[38] F.H. Sillinger, T.A. Weber, Computer simulation of local order in condensed phases of silicon, Phys. Rev. B. 31 (1985) 5262–5271. doi:10.1103/PhysRevB.31.5262.

[39] J.J. Wortman, R.A. Evans, Young's modulus, shear modulus, and poisson's ratio in silicon and germanium, J. Appl. Phys. 36 (1965) 153–156. doi:10.1063/1.1713863.

[40] E. Bitzek, P. Koskinen, F. Gähler, M. Moseler, P. Gumbsch, Structural Relaxation Made Simple, Phys. Rev. Lett. 97 (2006) 170201. doi:10.1103/PhysRevLett.97.170201.

[41] E. Mandenci, I. Guven, The finite element method and applications in engineering using ANSYS, Springer, 2006.

[42] P. Lazzarin, F. Berto, Control volumes and strain energy density under small and large scale yielding due to tension and torsion loading, Fatigue Fract. Eng. Mater. Struct. 31 (2008) 95–107. doi:10.1111/j.1460-2695.2007.01206.x.

[43] F. Berto, P. Lazzarin, Recent developments in brittle and quasi-brittle failure assessment of

engineering materials by means of local approaches, Mater. Sci. Eng. R Reports. 75 (2014) 1–48. doi:10.1016/j.mser.2013.11.001.

[44] R. Pippan, S. Wurster, D. Kiener, Fracture mechanics of micro samples: Fundamental considerations, Mater. Des. 159 (2018) 252–267. doi:10.1016/j.matdes.2018.09.004.

[45] A.R. Torabi, F. Berto, Fracture Assessment of Blunt V-Notched Graphite Specimens by Means of the Strain Energy Density, Strength Mater. 45 (2013) 635–647. doi:10.1007/s11223-013-9500-z.

[46] M.R. Ayatollahi, F. Berto, A. Campagnolo, P. Gallo, K. Tang, Review of local strain energy density theory for the fracture assessment of V-notches under mixed mode loading, Eng. Solid Mech. 5 (2017) 113–132. doi:10.5267/j.esm.2017.3.001.

[47] P. Lazzarin, F. Berto, M. Elices, J. Gómez, Brittle failures from U- and V-notches in mode I and mixed, I + II, mode: a synthesis based on the strain energy density averaged on finite-size volumes, Fatigue Fract. Eng. Mater. Struct. 32 (2009) 671–684. doi:10.1111/j.1460-2695.2009.01373.x.

[48] Z.P. Bažant, J. Ožbolt, Nonlocal Microplane Model for Fracture, Damage, and Size Effect in Structures, J. Eng. Mech. 116 (1990) 2485–2505. doi:10.1061/(ASCE)0733-9399(1990)116:11(2485).

[49] Z.P. Bažant, M. Jirásek, Nonlocal Integral Formulations of Plasticity and Damage: Survey of Progress, J. Eng. Mech. 128 (2002) 1119–1149. doi:10.1061/(ASCE)0733-9399(2002)128:11(1119).

[50] P. Gallo, T. Sumigawa, T. Shimada, Y. Yan, T. Kitamura, Investigation into the Breakdown of Continuum Fracture Mechanics at the Nanoscale: Synthesis of Recent Results on Silicon, in: E.E. Gdoutos (Ed.), Proc. First Int. Conf. Theor. Appl. Exp. Mech., Springer International Publishing, Cham, 2019: pp. 205–210. doi:10.1007/978-3-319-91989-8_45.

[51] L. Guo, T. Kitamura, Y. Yan, T. Sumigawa, K. Huang, Fracture mechanics investigation on crack propagation in the nano-multilayered materials, Int. J. Solids Struct. 64–65 (2015) 208–220. doi:10.1016/j.ijsolstr.2015.03.025.

[52] T. Sumigawa, S. Ashida, S. Tanaka, K. Sanada, T. Kitamura, Fracture toughness of silicon in nanometer-scale singular stress field, Eng. Fract. Mech. 150 (2015) 161–167. doi:10.1016/j.engfracmech.2015.05.054.